

# EFFECT OF SOURCE VOLTAGE SUBHARMONICS ON A RAPID CYCLING SYNCHROTRON POWER SUPPLY

F.Q. Zhang, The Graduate Univ. for Advanced Studies, KEK, Tsukuba, Japan  
T. Adachi and K. Endo, High Energy Accelerator Research Organization, KEK, Tsukuba, Japan

Abstract

In a 50 Hz rapid cycling power supply, the resonant ac current of the synchrotron magnet is modulated by the subharmonics of the source voltage rectified in 12 pulses with SCR. The modulation is found to be caused by the fluctuation of the pulsed power that is transferred to the magnet circuit via a choke transformer due to the cycle-to-cycle unequal charging of the capacitor located just after the rectifier. This phenomena is observed when there is a mismatch between frequencies of the power line and resonant magnet circuit. In this paper, the modulation behavior is analyzed and the experimental results are given as well as those of the circuit computations.

## 1 INTRODUCTION

In fast-cycling synchrotrons, a pulsed power supply is commonly used as power source for resonant network as shown in Fig.1.

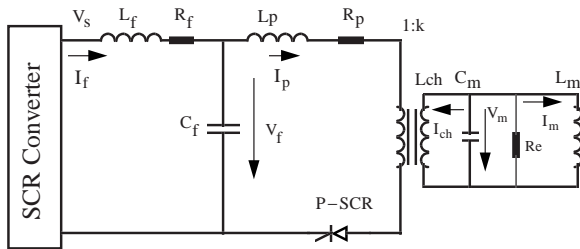


Figure 1: Pulsed power supply and resonant network for a fast cycling synchrotron.

Generally, the resonant magnet current is not easily affected by the source voltage disturbances owing to the large stored energy in the resonant network, but it is never immune from the disturbances. In a 50Hz rapid cycling power supply system [1, 2], modulation of the resonant current was observed and found to be caused by the harmonics, especially the subharmonics of the source voltage generated by a 12-pulse SCR rectifier. In this paper, the investigation on the effect of the source voltage on the resonant output is performed by both computation and experiment. To the best of our knowledge, the existing analyses [3, 4] were all carried out on an assumption of harmonics-free source voltage. This suggests a new approach that has to be developed to investigate the system response to source voltage harmonics. The approach described in this paper is based on the general method on the analysis of linear circuits containing periodically operated switches. The properties predicted by the computation are well justified by the experimental observations.

## 2 EFFECT OF SUBHARMONICS ON RESONANT CURRENT

The pulsed supply and its resonant network fit into the category of linear time-varying networks. Because of the periodical switching operation, the circuit reduces to the special class of linear, periodically time-varying networks. The response  $y(t)$  of a linear time varying system to an input  $x(t)$  with Fourier transform  $X(\omega)$  is defined by

$$y(t) = \frac{1}{2\pi} \int_{-\infty}^{\infty} H(\omega, t) X(\omega) e^{j\omega t} d\omega$$

where  $H(\omega, t)$  is the transfer function of the system [5]. For linear periodically time varying networks of period  $T$ , the system function is periodic with respect to the period  $T$ :  $H(\omega, t+T) = H(\omega, t)$ . Therefore, it may be expanded in a Fourier series,

$$H(\omega, t) = \sum_{n=-\infty}^{\infty} H_n(\omega) e^{j(2\pi n t/T)}$$

$H_0$  may be regarded as an averaged time varying system function. Evidently the remaining Fourier coefficients represent system responses at sidebands around  $n\omega_s = n(2\pi/T)$ . The analyses on periodically switched linear networks can be found in [6-9]. This paper follows Liou's approach [7]. We first present the system response to an sinusoidal or exponential input in time domain and describe the properties of the response. Then an analysis in frequency domain shows the sidebands containing in the pulse current  $I_p$  and resonant current  $I_m$ .

### 2.1 Time domain

#### 2.1.1 Approach

Generally the circuit can be described by the following differential equations with respect to the periods of switching-off and switching-on as follows,

$$\dot{X}_{n,k}(t) = A_k X_{n,k}(t) + B_k u(t) \quad (1.a)$$

$$y_{n,k}(t) = C_k X_{n,k}(t) + D_k u(t) \quad (1.b)$$

where  $X_{n,k}$  is a state vector,  $u$  an input vector,  $y_{n,k}$  an output vector,  $n$  the  $n$ -th operation and  $k=1, 2$  means the state of switching off and on, respectively. Fig.2 illustrates the notations for the  $n$ -th switching period.

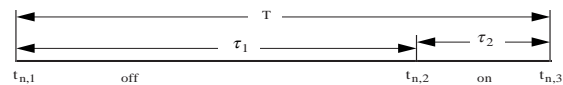


Figure 2: Notations for  $n$ -th switching period.

At the switching instants  $t_{n,2}$  and  $t_{n,3}$ , the boundary conditions can be described by the state transient matrices

$F_2$  and  $F_3$  as follows.

$$X_{n,2}(t_{n,2})=F_2X_{n,1}(t_{n,2})+G_2u(t_{n,2}) \quad (2.a)$$

$$X_{n+1,1}(t_{n,3})=F_3X_{n,2}(t_{n,3})+G_3u(t_{n,3}) \quad (2.b)$$

Assuming  $u(t)=ve^{pt}$ , where  $v$  is a constant and  $p$  is a complex number, the solution is given by

$$X_{n,k}(t) = \exp[A_k(t - t_{n,k})] \cdot [X_{n,k}(t_{n,k}) + \alpha_k(t_{n,k})] - \alpha_k(t) \quad (3.a)$$

$$\alpha_k(t) = (A_k - pI)^{-1} e^{pt} B_k v \quad (3.b)$$

The solution (3), together with (2) can be computed successively from a given initial vector to get the response, but a useful result about the boundary conditions is obtained as follows by manipulating further.

$$X_{n,1}(nT) = M^n [X_{0,1}(0) - Jv] + J e^{pnT} v \quad (4)$$

where  $J = [e^{pT} I - M]^{-1} H$ ,  $M = F_3 e^{A_2 \tau_2} F_2 e^{A_1 \tau_1}$  and

$$H = F_3 e^{A_2 \tau_2} F_2 (A_1 - pI)^{-1} (e^{A_1 \tau_1} - e^{pT_1}) B_1 + F_3 (A_2 - pI)^{-1} (e^{A_2 \tau_2} e^{p\tau_1} - e^{pT_2}) B_2 + F_3 e^{A_2 \tau_2} G_2 e^{p\tau_1} + G_3 e^{pT} \quad (6)$$

It is noticed from (4) that  $X_{n,1}(nT)$  consists of two terms. The first term represents the transient mode while the second is the steady-state mode. For  $n \rightarrow \infty$ ,  $M^n \rightarrow 0$  and we get the steady-state result,

$$X_{n,1}(nT)_{ss} = J e^{pnT} v. \quad (7)$$

From the repetitive computations of equations (2)-(7), the response in time domain is obtained.

## 2.1.2 Numerical results

### 2.1.2.1 System parameters

Considering the circuit of Fig.1, we have:

$$X_{n,1} = [i_f \quad v_f \quad i_L \quad v_m]^T \text{ and}$$

$$X_{n,2} = [i_f \quad v_f \quad i_p \quad i_L \quad v_m]^T,$$

where  $i_L = i_{ch} + i_m$ . In charging period ( $k=1$ ),

$$A_1 = \begin{bmatrix} -R_f/L_f & -1/L_f & 0 & 0 \\ 1/C_f & 0 & 0 & 0 \\ 0 & 0 & 0 & 1/L \\ 0 & 0 & -1/C_m & -1/(C_m R_e) \end{bmatrix}$$

$$B_1 = [1/L_f \quad 0 \quad 0 \quad 0]^T, \text{ and } i_p = 0.$$

In pulse period ( $k=2$ ),

$$A_2 = \begin{bmatrix} -R_f/L_f & -1/L_f & 0 & 0 & 0 \\ 1/C_f & 0 & -1/C_f & 0 & 0 \\ 0 & 1/L_p & -R_p/L_p & 0 & -1/(kL_p) \\ 0 & 0 & 0 & 0 & 1/L \\ 0 & 0 & 1/(kC_m) & -1/C_m & -1/(C_m R_e) \end{bmatrix}$$

$$B_2 = [1/L_f \quad 0 \quad 0 \quad 0 \quad 0]^T,$$

$$F_2 = \begin{bmatrix} 1 & 0 & 0 & 0 \\ 0 & 1 & 0 & 0 \\ 0 & 0 & 0 & 0 \\ 0 & 0 & 1 & 0 \\ 0 & 0 & 0 & 1 \end{bmatrix}, \quad F_3 = \begin{bmatrix} 1 & 0 & 0 & 0 & 0 \\ 0 & 1 & 0 & 0 & 0 \\ 0 & 0 & 0 & 1 & 0 \\ 0 & 0 & 0 & 0 & 1 \end{bmatrix}, \quad G_2 = 0 \text{ and}$$

$G_3 = 0$ , where  $L_f = 0.268H$ ,  $C_f = 0.6mF$ ,  $L_p = 1.86mH$ ,  $L_{ch} = 10.4mH$ ,  $L_m = 4.7mH$ ,  $L = L_{ch} L_m / (L_{ch} + L_m)$ ,  $R_f = 5m\Omega$ ,  $R_p = 1m\Omega$ ,  $k=2$ ,  $C_m = 3.2mF$ , and  $R_e \sim 70$ .  $R_e$  is a pseudo-resistance representing the ac loss. Accordingly, the resonant frequency (i.e. switching frequency) is  $f_s \sim 50Hz$ ,  $\tau_1 = 5\tau_2$  and  $\tau_1 + \tau_2 = T$  (=switching period). Resonant network quality factor is:  $Q = \omega_s C_m R_e \sim 70$ . The resonant condenser  $C_m$  is adjustable in both calculation and experiment for our purposes.

### 2.1.2.2 System response to source voltage harmonics

The source voltage is provided by a 12-pulse SCR rectifier, of which output contains both characteristic and non-characteristic harmonics that arise from "unideal" converter operation. The non-characteristic harmonics called subharmonics are the components with lower frequencies than the converter's fundamental frequency. Assuming the power line frequency  $f_0$ , the subharmonics are of frequencies  $hf_0$ , where  $h$  is an integer. For the model system under discussion,  $f_0 = 50Hz$  and  $h < 12$ . The calculation shows that the subharmonics appear as a modulation with frequency  $f_m = h\Delta f$  in resonant output as shown in Fig.3, where  $\Delta f = |f_s - f_0|$  and  $f_s$  is the switching frequency.

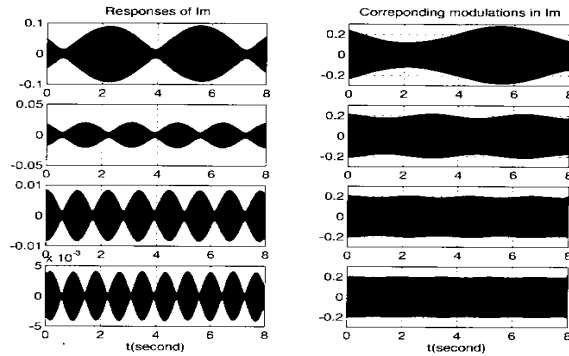


Figure 3: Modulations by subharmonics. Scaled responses (left) to unit amplitude with  $nf_0$  ( $n=1,2,3$  and 4 from top to bottom) in resonant current  $I_m$  for  $f_s = 49.85Hz$  are added to the unperturbed  $I_m$  in the exaggerated ways (right).

Modulation frequencies can be determined by investigating the variation mode in the boundary condition. For an input subharmonic  $v_s = e^{jh2\pi f_0 t}$  according to (7), the state vector is given at each beginning instant of switching period for steady-state operation as:

$$X_{n,1}(nT) = J e^{jh2n\pi f_0 / f_s}.$$

It is seen that  $X_{n,1}(nT)$  varies at a quasi-periodic mode with frequency  $f_m = h\Delta f$ , accordingly the system outputs will

also vary with the same way.  $f_m$  is not a rigid frequency but always holds a value close to  $h\Delta f$ .

## 2.2 Frequency domain

Frequency domain formulations are obtained by performing the Laplace transform of the state vector given by (3) then deriving the Laplace transformation for output  $y(t)$ . Finally the following results are obtained,

$$Y(s)|_{s=j\omega_0} = Y(\omega) = T(\omega) \frac{1}{j[\omega - (\omega_0 + n\omega_s)]} V,$$

$$T(\omega_0 + n\omega_s) = \sum_{k=1}^2 \{C_k e^{-j(\omega_0 + n\omega_s)\eta_k - 1} R_k(\omega_0 + n\omega_s) - \frac{e^{-jn\omega_s\eta_k - 1} (1 - e^{-jn\omega_s\tau_k})}{jn\omega_s} [C_k (A_k - j\omega_0 I)^{-1} B_k - D_k]\} / T$$

for  $n \neq 0$ , and

$$T(\omega_0) = \sum_{k=1}^2 \{C_k e^{-j\omega_0\eta_k - 1} R_k(\omega_0) - \tau_k [C_k (A_k - j\omega_0 I)^{-1} B_k - D_k]\} / T$$

for  $n=0$ , where  $\eta_0=0$  and  $\eta_1=\tau_1$ .  $R_k$  is complex matrix comprising the circuit configuration matrices and switching transformation matrices in (1) and (2), respectively. It is concluded that for a subharmonics  $hf_0$ , the output contains sidebands:  $nf_s \pm h\Delta f$  plus lower-frequency  $h\Delta f$ , where  $n=1,2,3,\dots$ . Fig.4 is a typical calculation result showing the spectra of  $I_p$ .

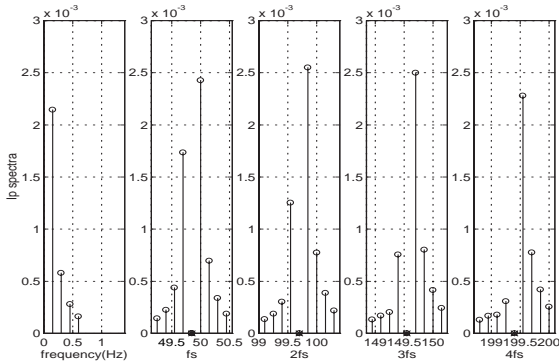


Figure 4: Calculated spectra of  $I_p$ ,  $f_s=49.85\text{Hz}$ .

## 3 EXPERIMENTS

The modulation in resonant current was measured and the relation to the subharmonics of 100Hz was obtained as in Fig.5. In the model pulsed power supply, the prominent subharmonic frequency is 100Hz due to the configuration

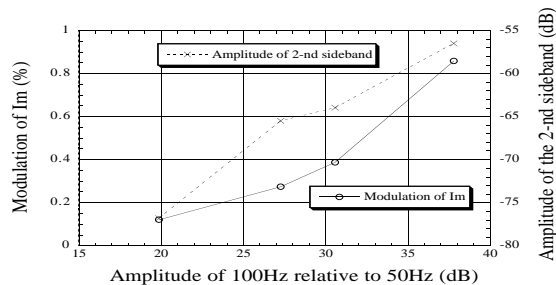


Figure 5: Modulation by 100Hz subharmonics

of the firing circuit for the 12-pulse rectifier, while 50Hz is very low and almost unchanged. The measured spectra of  $I_p$  and  $I_m$  in Fig.6 support the analyses made above. Sidebands of  $I_p$  appear at both sides of  $nf_s$  ( $n=1,2,\dots$ ), while those of  $I_m$  at both sides of only  $f_s$ . This is because the latter sidebands at higher frequency is suppressed by the decreased amplitude response of the transfer function of  $I_m/I_p$ .

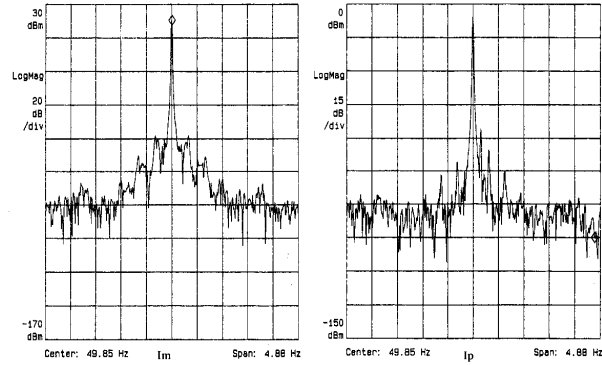


Figure 6: Measured spectra of  $I_p$  and  $I_m$ .

## 4 CONCLUSIONS

Analytical model based on the Liou's approach is used to adapt for the periodically operated SCR switch in the linear time-varying circuit whose frequency is different from the line frequency. This approach explains the experimental observations on the amplitude modulated ac current of the fast cycling synchrotron magnet quite well.

## 5 REFERENCES

- [1] K. Endo, Y. Ohsawa, W.M. Zhou and T. Yamagishi, "50Hz Power Supply for B-Factor Booster Synchrotron," 1993 IEEE Conf. Record Nuclear Science Symp. & Medical Imaging Conf., San Francisco, 1993, pp.385-9.
- [2] F.Q. Zhang K. Endo and Y. Irie, "Feedback Control of 50Hz Power Supply," EPAC96, Barcelona, 1996, pp.2343-5.
- [3] J.A. Fox, "Resonant magnet network and power supply for the 4 Gev electron synchrotron Nina," Proc. IEE Vol. 112, 1965, pp.1107-26.
- [4] A. Sreenivas e, G.G. Karaday and H.A. Thiessen, "A General Method for Resonance Power Supply Analysis," IEEE Trans., Vol. NS-39, 1992, pp.29-34.
- [5] M.R. Aaron, "Application characterization, and design of switched filters" in Modern Filter Theory and Design, G.C. Temes, and S.K. Titra. Eds. New York: John Wiley & Sons, Chap. 10.
- [6] W.R. Bennett, "Steady-state transmission through networks containing periodically operated switches." IRE Trans., Vol. CT-12, 1955, pp.17-21.
- [7] M.L. Liou, "Exact analysis of linear circuits containing periodically operated switches with applications," IEEE Trans., Vol. CT-19, pp.146-154.
- [8] T. Stroem and S. Signell, "Analysis of Periodically Switched Linear Circuits," IEEE Trans., Vol. CAS-24, 1977, pp.531-41.
- [9] A. Opal and J. Vlach, "Analysis and Sensitivity of Periodically Switched Linear Networks," IEEE Trans., Vol. CAS-36, 1989, pp. 522-32.